Journal of Modern Optics
Publication details, including instructions for authors and subscription information:
http://www.tandfonline.com/loi/tmop20

Quantitative imaging and measurement of cell-substrate surface deformation by digital holography

Xiao Yu [a], Michael Cross [b], Changgeng Liu [a], David C. Clark [a], Donald T. Haynie [b] & Myung K. Kim [a]

[a] Digital Holography and Microscopy Laboratory, Department of Physics, University of South Florida, Tampa, FL 33620, USA

[b] Nanomedicine and Nanobiotechnology Laboratory, Department of Physics, University of South Florida, Tampa, FL 33620, USA

Version of record first published: 25 Sep 2012.

To cite this article: Xiao Yu, Michael Cross, Changgeng Liu, David C. Clark, Donald T. Haynie & Myung K. Kim (2012): Quantitative imaging and measurement of cell-substrate surface deformation by digital holography, Journal of Modern Optics, 59:18, 1591-1598

To link to this article: http://dx.doi.org/10.1080/09500340.2012.729095

Journal of Modern Optics
Vol. 59, No. 18, 20 October 2012, 1591–1598

Taylor & Francis
Taylor & Francis Group

Quantitative imaging and measurement of cell–substrate surface deformation by digital holography

Xiao Yu[a], Michael Cross[b], Changgeng Liu[a], David C. Clark[a], Donald T. Haynie[b] and Myung K. Kim[a]*

[a]*Digital Holography and Microscopy Laboratory, Department of Physics, University of South Florida, Tampa, FL 33620, USA;* [b]*Nanomedicine and Nanobiotechnology Laboratory, Department of Physics, University of South Florida, Tampa, FL 33620, USA*

(*Received 4 May 2012; final version received 1 September 2012*)

Quantitative phase microscopy by digital holography (DH-QPM) is introduced to study the cell–substrate interactions and migratory behavior of adhesive cells. A non-wrinkling elastic substrate, collagen-coated polyacrylamide (PAA) has been employed and its surface deformation due to cell adhesion and motility has been visualized as certain tangential and vertical displacement and distortion. The surface deformation on substrates of different elasticity and thickness has been quantitatively imaged and the corresponding cellular traction force of motile fibroblasts has been measured from phase profiles by DH-QPM. DH-QPM is able to yield quantitative measures directly and provide efficient and versatile means for quantitatively analyzing cellular motility.

Keywords: digital holography; quantitative phase microscopy; cell–substrate deformation; traction force

1. Introduction

The locomotion of cells typically takes place with the protrusion at the front end of the cells, followed by the formation of new adhesion near the site of protrusion on the underlying substrate. Then cells detach or retract their trailing end from the substrate, appearing as a contraction along the cell body. This kind of retraction turns out to be a forward movement. During the locomotion, cells detect their physical environment by applying traction forces to the substrate and then obtaining mechanical feedback only at the cell–substrate contact points, known as focal adhesions [1]. In the field of cellular biomechanics, theoretical and computational models of cells attached to an elastic substrate employed a finite element method (FEM) [2] to indicate that the cell–substrate interface deforms both tangentially and vertically. The adhesion site displacement decays within the length scale of the cell boundary ~40 μm and the minimum gel thickness (critical thickness) at which cells start to sense the rigid base below the gel is suggested to be 1.5–2 μm [3]. Quantitative phase microscopy by digital holography (DH-QPM) has been applied to quantitatively image and analyze living cells in a three-dimensional (3-D) collagen matrix [4,5]. Phase profiles of the shape change of cardiomyocytes have been evaluated to yield quantitative parameters characterizing the cell dynamics [6]. The traction forces exerted by fibroblasts cultured on a silicone rubber substrate have been visualized as an elastic distortion and wrinkling by DH-QPM [7]. Quantitative imaging of wrinkles on silicone rubber due to cell adhesion and motility has been performed. We have detected the cellular forces and quantified variations in force within the adhesion area of a cell over time. The traction force has been measured as $\sim 4 \times 10^{-3}$ dyn/cell based on the degree of wrinkling determined from phase information. DH-QPM is shown to be an effective approach for measuring the traction forces of cells cultured on the silicone rubber substrate.

Harris et al. has indicated that cells crawling on the substrate exerted traction as a shearing force in the plane of the plasma membrane surface closest to the substrate [8]. It is worth mentioning wrinkling is thought to be more elastic than plastic. If cells detach the substrate, wrinkles will disappear and a flat surface is restored. One may suspect that substrate elasticity will be incomplete and deformation is not entirely linear when forces are applied at multiple locations on the substrate. To address these issues, a non-wrinkling substrate, collagen-coated polyacrylamide (PAA) was applied to make direct measurement of elastic deformations, albeit at discrete locations [9]. The technique of using collagen-coated polyacrylamide as the non-wrinkling elastic substrate with embedded microspheres has been employed to study effects of substrate

*Corresponding author. Email: mkkim@usf.edu

ISSN 0950–0340 print/ISSN 1362–3044 online

http://dx.doi.org/10.1080/09500340.2012.729095
http://www.tandfonline.com

rigidity on cell movement [10], measure traction force of cells and allow the deformation with a significantly larger range of stress [9]. The advantage of PAA is that its elasticity, such as stiffness (Young's modulus E), can be adjusted by controlling the concentrations of the monomer and cross-linker. When cells are cultured on substrates of identical chemical properties but different rigidities, they are able to detect and respond to substrate stiffness by showing various motility pattern and morphologies [11]. The substrate then generates deformation due to the traction forces exerted by cells. In general, cells generate more traction force on substrate with higher elasticity. Measurements of the traction force of biological cells have been previously made using various methods, such as measurement of the displacements of embedded marker beads [9,12] and hydrostatic pressure applied through micropipette [13]. Also, the mechanical properties of a substrate have been characterized by methods such as atomic force microscopy [14] or manipulation of spherical beads [15]. Compared to these approaches, DH-QPM is able to yield quantitative measures of deformation directly. We have utilized DH-QPM to measure the Young's modulus of PAA [16], which provided a very effective process for achieving high-precision quantitative phase microscopy compared to other methods of measuring deformation of soft materials. Here, DH-QPM has been used to visualize cell–substrate adhesion and extract quantitative measures of surface deformation. The substrate stiffness and quantitative measures of substrate deformation have been combined to produce estimates of the traction forces and characterize how these forces vary depending on the substrate rigidity.

2. Experiments

2.1. DHM setup

The DHM setup used in this work is illustrated in Figure 1 [7]. It consists of a Mach–Zehnder interferometer illuminated with a He–Ne laser whose wavelength is 633 nm. The object arm contained a sample stage and a microscope objective (MO1) that projected a magnified image of the object onto a CCD camera. The reference arm similarly contained another objective MO2, so that the holographic interference pattern contained fringes due to interference between the diffracted object field and the off-axis reference field. The numerical aperture (NA) of the microscope objectives is 0.25 and the magnification is 10×. The specification of CCD is 1024 × 768, and the pixel size is 4.65 μm. The QPM images were reconstructed from the captured holograms by the angular spectrum method [17,18]. Aberrations and background distortions of the optical field were minimized by available DHM techniques [17,18]. LED illumination from above BS1 provided a means of acquiring a bright-field (non-interferometric) microscopy image of the specimen. A hood with a heater inside covers the entire setup to keep the environment temperature as 37°C.

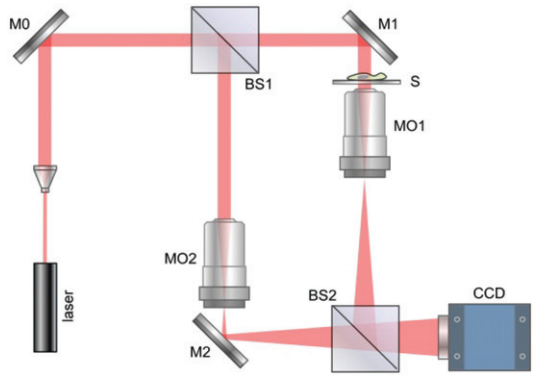

Figure 1. DHM setup: Ms, mirrors; BSs, beam splitters; MOs, microscope objectives; S, sample object. (The color version of this figure is included in the online version of the journal.)

2.2. Cell–substratum samples

The cell–substratum samples consisted of fibroblast cells cultured on a thin layer of soft or stiff collagen-coated PAA. The PAA film was made from polyacrylamide prepolymer prepared as described in [19]. The flexibility of the substrate was manipulated by adjusting the concentrations of acrylamide and bis-acrylamide. PAA samples with different Young's moduli and thickness were prepared on a square coverglass (25 mm × 25 mm) by varying the acrylamide concentration between 5% and 8% and bis-acrylamide between 0.1% and 0.03%. The Young's moduli of these samples (acrylamide 5%, bis 0.1% and acrylamide 8%, bis 0.03%) were 28 kPa and 14 kPa, measured by DHM setup [16]. The thickness was controlled to be 40 μm, 78 μm, and 200 μm by varying the volumes of the acrylamide and bis-acrylamide solution and the size the coverglass on the top of the gel. Cells culture was described in [7]. Approximately 10^4 normal human dermal fibroblasts (NHDF) were seeded onto a coverglass in a Petri dish prepared as described above, culture medium was added, and the Petri dish was covered and incubated at 37°C and 5% CO_2.

The scheme of cells on PAA substrate is shown in Figure 2(*a*). Comparing to our previous study of silicone rubber substrate (Figure 2(*b*)), the patterns of cells deforming the substrates coupled with corresponding optical thickness are shown as displacement

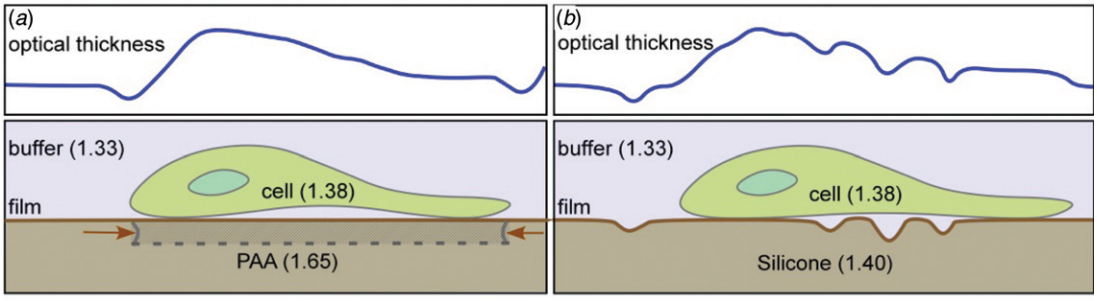

Figure 2. Schematics of the cell–substrate samples (lower) for (*a*) PAA and (*b*) silicone, and the corresponding optical thickness profiles (upper). The cell–silicone sample was taken from [7] for comparison. (The color version of this figure is included in the online version of the journal.)

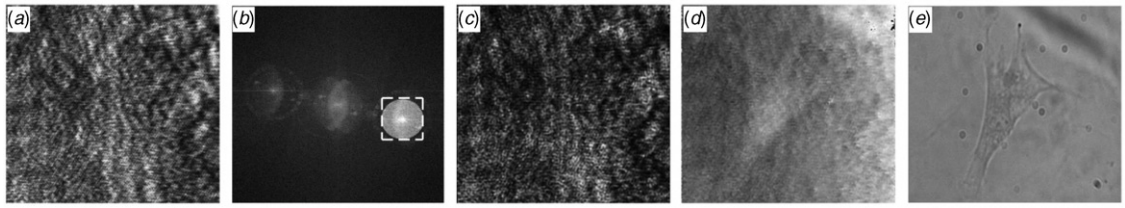

Figure 3. DHM analysis of fibroblasts deforming PAA substrate. The field of view is $190 \times 176\,\mu m^2$ with 800×742 pixels: (*a*) hologram; (*b*) angular spectrum; (*c*) amplitude image; (*d*) quantitative phase image; (*e*) bright field image.

and distortion tangentially and vertically due to traction force exerted by cells for PAA instead of wrinkles for silicone rubber substrate.

2.3. DHM analysis

DHM analysis of fibroblasts deforming the PAA substrate (Figure 3) is based on the method similar to analyzing cells wrinkling a silicone rubber film [7]. Figure 3(*a*) shows the hologram generated by the interference of the diffracted object field and off-axis reference field. In Figure 3(*b*), the angular spectrum shows the zero-order and a pair of first-order components. One of the first-order components was separated with a numerical band-pass filter when the off-axis angle of the reference beam was properly adjusted. The corresponding amplitude and the phase profile after correct centering of the filtered angular spectrum and numerical propagation to the object focus distance are shown in Figure 3(*c*) and (*d*). For comparison, Figure 3(*e*) shows the bright field image for LED illumination, slightly defocused to make the transparent structures visible.

2.4. Principle of force estimation

Figure 4 shows a sketch of a cell deforming the substrate horizontally, where F is the traction force of the cell; d is the physical thickness of the deformed underlying substrate; L_0 and L_1 are the length of the deformed underlying substrate before and after the deformation due to the traction force exerted by cell; A_0 is the effective cross-section area and M is the corresponding mass of the deformed substrate. The traction force by the cells was estimated by the following algorithm. The density of substrate is $\rho_0 = \frac{M}{A_0 L_0}$ before the deformation and $\rho_1 = \frac{M}{A_0 L_1}$ after the deformation, which is expressed as $\rho_0 L_0 = \rho_1 L_1$. Then the length difference is $\frac{\Delta L}{L_0} = \frac{L_0 - L_1}{L_0} = 1 - \frac{\rho_0}{\rho_1}$.

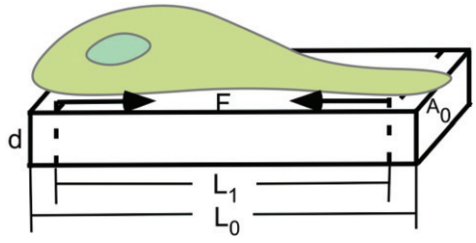

Figure 4. Sketch of a cell-deformed substrate in the horizontal direction: F is the traction force of the cell; d is the physical thickness of the deformed underlying substrate; L_0 and L_1 are the lengths of the deformed underlying substrate before and after the deformation due to the traction force exerted by cell; A_0 is the side area of the deformed substrate; M is the corresponding mass of the deformed substrate. (The color version of this figure is included in the online version of the journal.)

Combining with the optical thickness extracted from the phase profile, the index change due to the deformation is $\Delta n = n_1 - n_0 = \frac{\lambda\Delta\phi}{2\pi d}$, where $\lambda = 0.633\,\mu m$ and $n_0 = 1.65$ in our case [16]. d, known as critical thickness in literature through which cells can feel an underlying rigid base below the elastic substrate, was estimated to be $\sim 2\,\mu m$ [3]. The degree of deformation cells produced on substrate $\Delta\phi$ was extracted from the phase profile. The relation between the density and index of the substrate is $\frac{\rho_0}{\rho_1} = \frac{n_0 - 1}{n_1 - 1}$. From the definition of Young's modulus E, the traction force in the form of stress is expressed as $\frac{F}{A_0} = \frac{E\Delta L}{L_0}$.

3. Results and discussion

3.1. Examples of fibroblasts deforming the PAA

Examples of fibroblasts deforming the PAA gel film are presented in Figure 5(*a–d*) and (*e–h*). The Young's moduli of the PAA substrate are 28 kPa and 14 kPa, and the thicknesses are both 78 μm. For the purpose of comparison, an example of fibroblasts wrinkling a silicone rubber film is also presented (Figure 5(*i–l*) [7]). The field of view was $190 \times 176\,\mu m^2$ with 800×742 pixels in all the cases. Figure 5(*a*, *e*, *i*) shows bright-field images for LED illumination, slightly defocused to make the transparent structures visible. Figure 5(*a*, *e*) show a single cell crawling on the flat PAA film surface without any wrinkles, while several cells and also a few prominent wrinkles are shown in Figure 5(*i*).

Figure 5(*b*, *f*, *j*) presents quantitative phase images by DH-QPM, where the full range of the gray scale values, from black to white, covers the phase variation 0–2π. The deformation area appears as dark shadow around the cell body because the substrate surface was deformed by certain tangential and vertical displacement and distortion due to the traction forces exerted by cells. This is consistent with the depiction in Figure 2. Figure 5(*c*, g, *k*) is the optical thickness profiles corresponding to the highlighted lines AB, CD and EF in Figure 5(*b*, *f*, *j*). G and H are the deformation areas on PAA across the cell body and I is the winkling area of cells on silicone rubber film. In fact, the graphs of Figure 5(*c*, *g*, *k*) plot profiles along

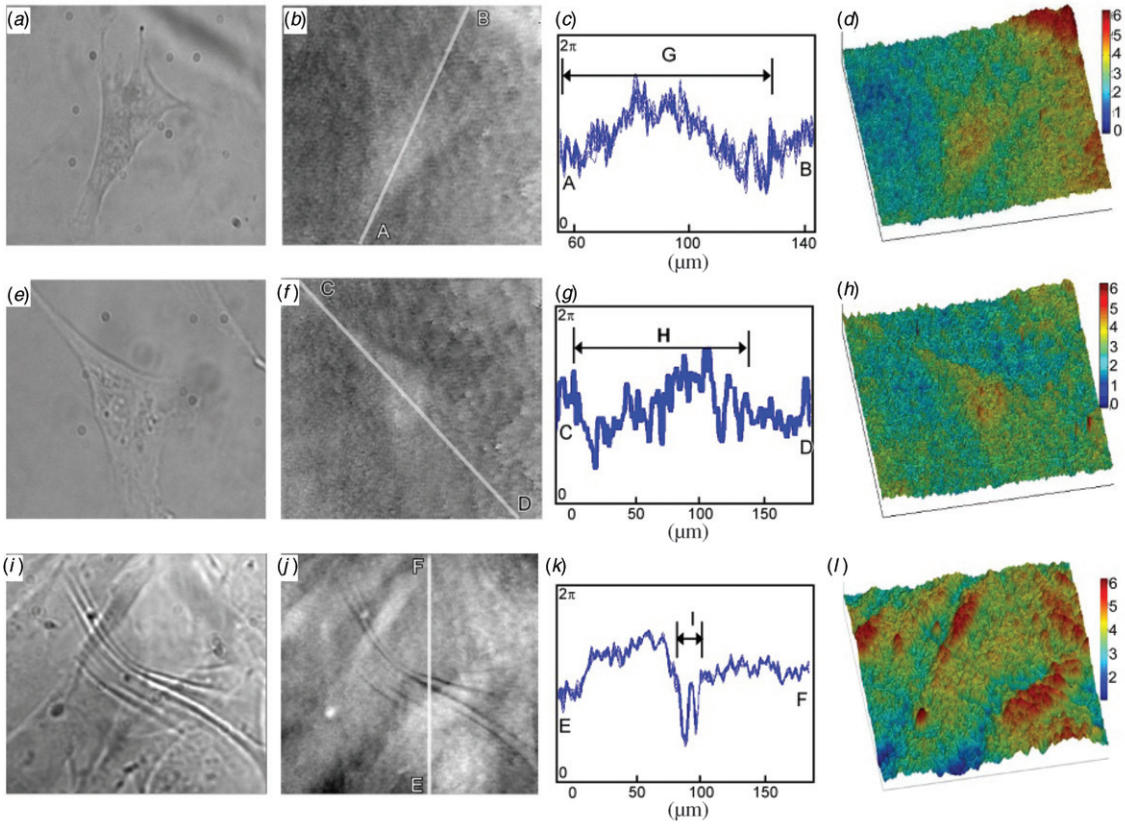

Figure 5. (*a–d*) Cells deforming a PAA film (Young's modulus of PAA substrate is 28 kPa; thickness is 78 μm); (*e–h*) cells deforming a PAA film (Young's modulus of PAA substrate is 14 kPa; thickness is 78 μm); (*i–l*) cells wrinkling a silicone rubber film. (*a, e, i*) Bright field images; (*b, f, j*) quantitative phase images; (*c*, *g*, *k*) cross-sections of phase profiles along highlighted lines AB in (*b*), CD in (*f*) and EF in (*j*); (*d*, *h*, *l*) pseudo-color 3D rendering of phase images (*b*, *f*, *j*). The field of view was $190 \times 176\,\mu m^2$ with 800×742 pixels. (The color version of this figure is included in the online version of the journal.)

10 adjacent vertical lines, to indicate the general noise level. Most of the 'fluctuations' appear to be non-random between adjacent lines, and the noise level is seen to be less than 0.1 radian. The optical thickness represents the combined effect of the physical thickness and the refractive index. For example, the upward bump in the area G is due to the presence of a cell body (average index 1.38) attached to the PAA substrate (1.65). For the phase difference a $\Delta\varphi = 1.0$ radian phase jump in this case corresponds to physical thickness of the cell $h = 0.4\,\mu\text{m/rad}$. On the other hand, for the wrinkles in area I, the relevant index difference is $n_1 - n_2 = 1.40 - 1.33 = 0.07$, and the physical depth of the wrinkle is $h = 1.4\,\mu\text{m/rad}$. Figure 5(*d*, *h*, *l*) is pseudo-color pseudo-3D rendering of the phase images in Figure 5(*b*, *f*, *j*), providing intuitive visualization of the cell and substrate.

3.2. Phase movie of fibroblasts deforming PAA

We recorded a time-lapse phase movie (see Media 1 online) of the migration of cells every 3 min over a period of 2 h. To minimize the effects of intercellular mechanical interactions through the elastic substrate, we focused on individual cells without neighbors in the field of view. An individual cell in Figure 6 was seen to spread and crawl on the PAA surface, changing its shape and orientation. The overall area of the cell changed as it formed protrusions at the leading edge. The traction force compressed the PAA film and stretched it, forming dark shadow in the surrounding area.

3.3. Force estimation

The traction forces of cells cultured on the PAA substrate of various thicknesses for two different Young's moduli E are shown in Figures 7 and 8. For brevity, the following descriptions of the estimation of the traction force of cells refer to the first example in which the Young's modulus of the PAA substrate is 14 kPa and the thickness is 40 μm (Figure 7(*a–c*)). Figure 7(*c*) presents the optical thickness corresponding to the highlighted line in Figure 7(*b*), and the length of the arrow indicates the phase variation of the deformation area and the surrounding noise level provides the estimation of the error $\Delta\phi = 1.27 \pm 0.64$ rad. The index change is $\Delta n = n_1 - n_0 = \frac{\lambda\Delta\phi}{2\pi d} = 0.06$ [3], and we obtained $n_1 = 1.71$, $\frac{\rho_0}{\rho_1} = \frac{n_0 - 1}{n_1 - 1} = 0.91$, thus $\frac{\Delta L}{L_0} = \frac{L_0 - L_1}{L_0} = 1 - \frac{\rho_0}{\rho_1} = 0.09$ and the traction force in the form of stress with the error estimation $\frac{F}{A_0} = \frac{E\Delta L}{L_0} = 12.57 \pm 6.18\,\text{kdyn/cm}^2$. Similarly, in Figure 7(*d–f*) and (*g–i*), for which Young's moduli are both 14 kPa while the thicknesses are 78 μm and 200 μm, respectively, the phase variations of the deformation areas are $\Delta\phi = 1.25 \pm 0.63$ rad and 1.29 ± 0.50 rad. These results show that cells cultured on PAA substrate of identical Young's modulus but different thickness generated similar phase variation, which can reveal the traction force of cells. The traction forces are then estimated to $12.37 \pm 6.18\,\text{kdyn/cm}^2$ and $12.75 \pm 5.19\,\text{kdyn/cm}^2$, almost identical values (Table 1).

Figure 8 shows another example of cells cultured on PAA substrate whose Young's modulus is 28 kPa and the thicknesses are also 40 μm, 78 μm and 200 μm. We applied the same method to extract the phase variation and estimate the traction force, i.e. $\Delta\phi = 1.00 \pm 0.36$ rad, 0.99 ± 0.33 rad and 1.04 ± 0.46 rad for Figure 8(*a–c*), (*d–f*) and (*g–i*). The corresponding traction forces are estimated to be $20.19 \pm 7.56\,\text{kdyn/cm}^2$, $20.04 \pm 7.10\,\text{kdyn/cm}^2$ and $20.93 \pm 9.52\,\text{kdyn/cm}^2$ (Table 1).

Our experimental results show that the traction forces cells exerted on PAA substrate are independent of the thickness but increase with the Young's modulus of the substrate. This is consistent with the model of Maloney et al. [3] and the experimental results of Merkel et al. [20]. Our results for NHDFs can be compared with the measured traction forces 10.9 kdyn/cm^2 and 6.2 kdyn/cm^2 for the 3T3 fibroblasts on PAA substrate of Young's modulus 30 kPa and 14 kPa in [10].

Some issues and possible improvements of the technique are worth mentioning. The overlap of the cell body and intra- and extra-cellular particulate matter in the middle of the deformation would invalidate the phase difference calculation. An improved method total internal reflection (TIR) digital

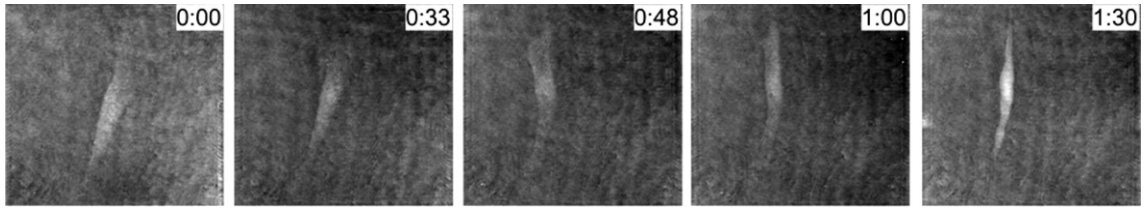

Figure 6. An excerpt of several frames from phase movie recordings of cells deforming PAA (Media 1). The field of view was $190 \times 176\,\mu\text{m}^2$ with 800×742 pixels. Time interval of two contiguous images above was around 30 min.

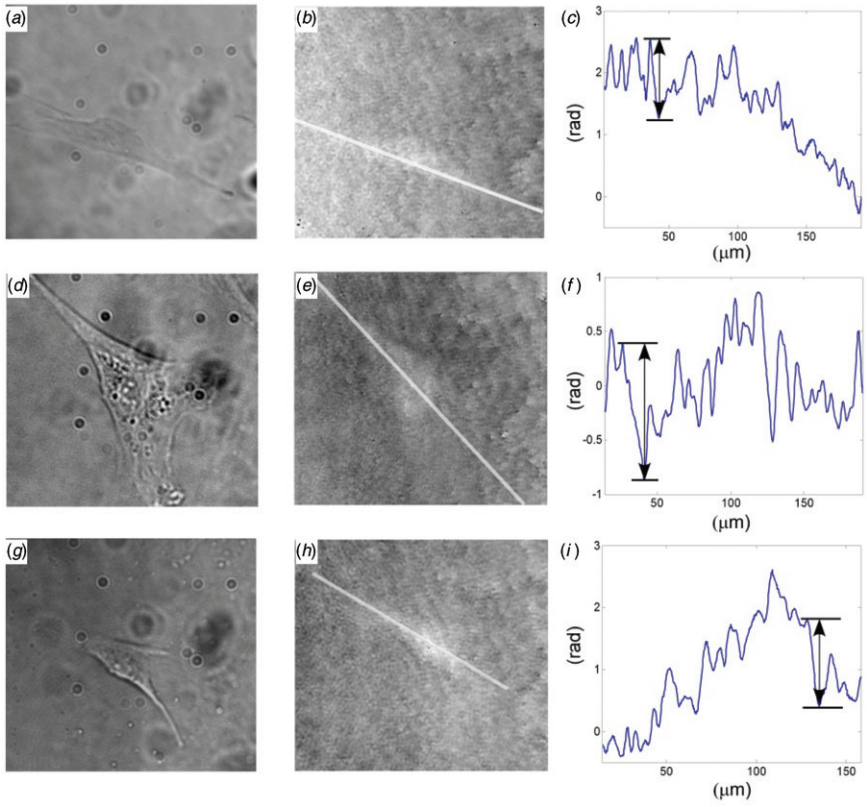

Figure 7. Cells cultured on the PAA substrate of Young's modulus 14 kPa. The thicknesses of the substrate are 40 μm, 78 μm and 200 μm for the three panels. (*a*, *d*, *g*) Bright field images; (*b*, *e*, *h*) quantitative phase images; (*c*, *f*, *i*) cross-sections of phase profiles along highlighted lines in phase images. The field of view was $190 \times 176\,\mu m^2$ with 800×742 pixels. (The color version of this figure is included in the online version of the journal.)

holography [21,22], which can reveal the wrinkle or deformation profiles only, without interference or noise of the cell bodies or spurious debris and inhomogeneities of the buffer solution, may provide a better method in our future cell-substrate study.

4. Conclusions

DH-QPM has been applied to quantitative imaging of fibroblasts deforming a non-wrinkling substrate collagen-coated PAA. The traction forces exerted by fibroblasts cultured on PAA substrate have been visualized as tangential and vertical deformation, compared to wrinkles on silicone rubber. The traction force has been measured based on the degree of deformation determined from phase information and shown to be independent of the thickness but increase with the Young's modulus of the substrate. DHM is an emergent imaging technology of new paradigm, with many novel capabilities and techniques. DH-QPM which is an important aspect of DHM can generate profiles of optical thickness with nanometer or even sub-nanometer precision, and the complex optical fields can be numerically manipulated in ways that are not feasible in real space holography. Current methods of measuring the traction forces of cells on elastic substrate such as cell-populated collagen gel in which cells are mixed with collagen gel as a disk, and the traction forces are estimated by the change in diameter of the disk [23–25]; force sensor array which uses a micro-machined device consisting of an array of cantilever beams that is fabricated using lithography [26]; employing fluorescent microbeads as markers for tracking the movement of the substrate under the traction forces of cells which are then computed by corresponding mathematical algorithm [9,27,28]. Compared to these methods, DH-QPM is able to provide direct access to the quantitative measures of the substrate elasticity and sensitive to cellular forces, so that it can detect and quantify variations in force within the adhesion area of a cell over time. DH-QPM is shown to be an effective approach for measuring the traction forces of cells and analyzing the cells motility.

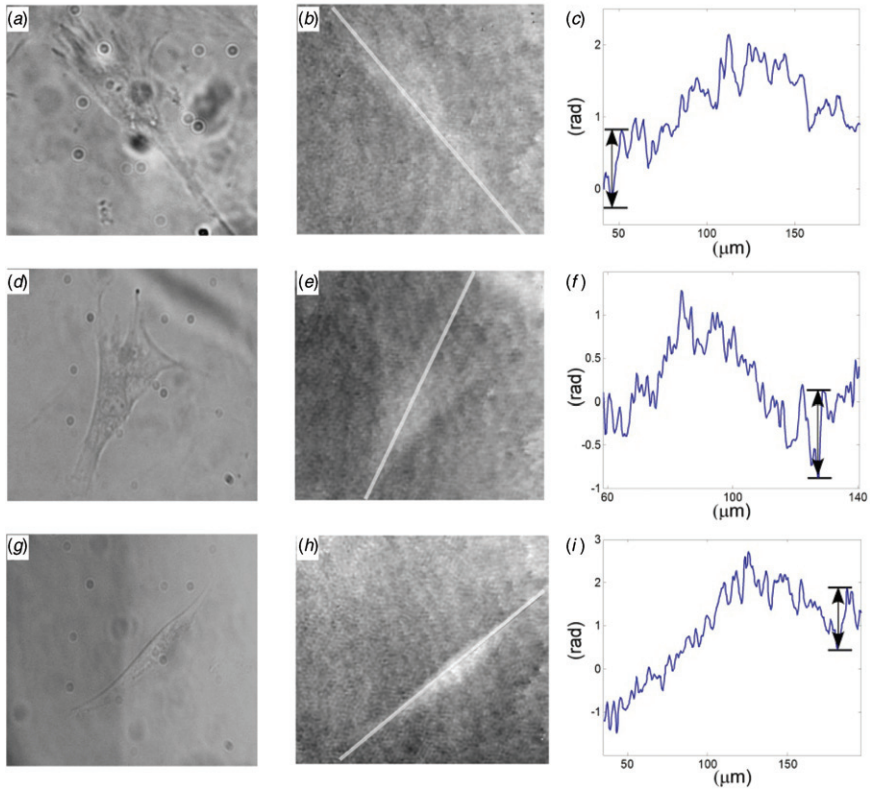

Figure 8. Cells cultured on the PAA substrate of Young's modulus 28 kPa. The thicknesses of the substrate are 40 μm, 78 μm and 200 μm for the three panels. (*a*, *d*, *g*) Bright field images; (*b*, *e*, *h*) quantitative phase images; (*c*, *f*, *i*) cross-sections of phase profiles along highlighted lines in phase images. The field of view was $190 \times 176\,\mu m^2$ with 800×742 pixels. (The color version of this figure is included in the online version of the journal.)

Table 1. Summary of Young's modulus and thickness of PAA, phase changes and traction forces of cells.

E (kPa)	Thickness (μm)	$\Delta\phi$(rad)	F/A_0 (kdyn/cm^2)
14	40	1.27 ± 0.64	12.57 ± 6.18
	78	1.25 ± 0.63	12.37 ± 6.18
	200	1.29 ± 0.50	12.75 ± 5.19
28	40	1.00 ± 0.36	20.19 ± 7.56
	78	0.99 ± 0.33	20.04 ± 7.10
	200	1.04 ± 0.46	20.93 ± 9.52

References

[1] Discher, D.E.; Janmey, P.; Wang, Y.L. *Science (Washington, DC, US)* **2005,** *310,* 1139–1143.

[2] Sen, S.; Engler, A.J.; Discher, D.E. *Cell. Mol. Bioeng.* **2009,** *2,* 39–48.

[3] Maloney, J.M.; Walton, E.B.; Bruce, C.M.; Vliet, K.J. *Phys. Rev. E: Stat., Nonlinear, Soft Matter Phys.* **2008,** *78,* 041923.

[4] Dubois, F.; Yourassowsky, C.; Monnom, O.; Legros, J.C.; Debeir, O.; Van Ham, P.; Kiss, R.; Decaestecker, C. *J. Biomed. Opt.* **2006,** *11,* 054032.

[5] Langehanenberg, P.; Ivanova, L.; Bernhardt, I.; Ketelhut, S.; Vollmer, A.; Dirksen, D.; Georgiev, G.; von Bally, G.; Kemper, B. *J. Biomed. Opt.* **2009,** *14,* 014018.

[6] Shaked, N.T.; Satterwhite, L.L.; Bursac, N.; Wax, A. *Biomed. Opt. Express* **2010,** *1,* 706–719.

[7] Yu, X.; Cross, M.; Liu, C.; Clark, D.C.; Haynie, D.T.; Kim, M.K. *Biomed. Opt. Express* **2012,** *3,* 153–159.

[8] Harris, A.K.; Wild, P.; Stopak, D. *Science (Washington, DC, US)* **1980,** *208,* 177–179.

[9] Dembo, M.; Wang, Y.L. *Biophys. J.* **1999,** *76,* 2307–2316.

[10] Lo, C.M.; Wang, H.B.; Dembo, M.; Wang, Y.L. *Biophys. J.* **2000,** *79,* 144–152.

[11] Pelham Jr, R.J.; Wang, Y.L. *Proc. Natl. Acad. Sci. USA* **1997,** *94,* 13661–13665.

[12] Oliver, T.; Lee, J.; Jacobson, K. *Semin. Cell Biol.* **1994,** *5,* 139–147.

[13] Usami, S.; Wung, S.L.; Skieczynski, B.A.; Skalak, R.; Chien, S. *Biophys. J.* **1992,** *63,* 1663–1666.

[14] Dimitriadis, E.K.; Horkay, F.; Maresca, J.; Kachar, B.; Chadwick, R.S. *Biophys. J.* **2002,** *82,* 2798–2810.

[15] Lin, D.C.; Yurke, B.; Langrana, N.A. *J. Biomech. Eng.* **2005,** *127,* 571–579.

[16] Yu, X.; Liu, C.; Clark, D.C.; Kim, M.K. In *Digital Holography and Three-dimensional Imaging*; OSA

Technical Digest (CD); Optical Society of America, 2011; Paper DTuC32.
[17] Kim, M.K. *SPIE Rev*. **2010,** *1,* 1–50.
[18] Kim, M.K. *Springer Ser*. *Opt*. *Sci*. **2011,** *162,* 50–123.
[19] Wang, Y.L.; Pelham Jr, R.J. *Methods Enzymol*. **1998,** *298,* 489–496.
[20] Merkel, R.; Kirchgebner, N.; Cesa, C.M.; Hoffmann, B. *Biophys*. *J*. **2007,** *93,* 3314–3323.
[21] Ash, W.M.; Kim, M.K. *Opt*. *Express* **2008,** *16,* 9811–9820.
[22] Ash, W.M.; Krzewina, L.G.; Kim, M.K. *Appl*. *Opt*. **2009,** *48,* H144–H152.
[23] Bell, E.; Ivarsson, B.; Merrill, C. *Proc*. *Natl*. *Acad*. *Sci*. *USA* **1979,** *76,* 1274–1278.
[24] Ehrlich, H.P. *Prog*. *Clin*. *Biol*. *Res*. **1988,** *266,* 243–258.
[25] Moon, A.G.; Tranquillo, R.T. *AIChE J*. **1993,** *39,* 163–177.
[26] Galbraith, C.G.; Sheetz, M.P. *Proc*. *Natl*. *Acad*. *Sci*. *USA* **1997,** *94,* 9114–9118.
[27] Butler, J.P.; Tolic-Norrelykke, I.M.; Fabry, B.; Fredberg, J.J. *Am*. *J*. *Physiol*. *Cell Physiol*. **2002,** *282,* C595–C605.
[28] Yang, Z.; Lin, J.S.; Chen, J.; Wang, J.H. *J*. *Theor*. *Biol*. **2006,** *242,* 607–616.